Rationally designed squaryldiamides – a novel class of sugar-nucleotide mimics?†

Sven Niewiadomski,[a,c] Zeenat Beebeejaun,[a] Helen Denton,[b] Terry K. Smith,[b] Richard J. Morris[c] and Gerd K. Wagner*[a]

Received 16th March 2010, Accepted 12th May 2010
First published as an Advance Article on the web 7th June 2010
DOI: 10.1039/c004165c

Sugar-nucleotides such as GDP-mannose, GDP-fucose and UDP-glucose are important biomolecules with a central role in carbohydrate and glycoconjugate biosynthesis, metabolism and cell signalling. Analogues and mimics of naturally occurring sugar-nucleotides are sought after as chemical tools and inhibitor candidates for sugar-nucleotide-dependent enzymes including glycosyltransferases. Many sugar-nucleotides bind to their target glycosyltransferases *via* coordination of the diphosphate group to a divalent metal cofactor in the active site. The identification of uncharged, chemically stable surrogates for the diphosphate group, with the ability to coordinate to a divalent metal, is therefore an important design criteria for the development of sugar-nucleotide mimics. Here, we describe the rational design and synthesis of a novel class of sugar-nucleotide mimics based on a squaryldiamide scaffold, an uncharged phosphate isostere. We demonstrate by comprehensive NMR titration experiments that the new sugar-nucleotide mimics coordinate efficiently to Mg^{2+}, and provide results from biological studies with a therapeutically relevant mannosyltransferase from *Trypanosoma brucei*. Our findings suggest that squaryldiamides are a promising template for the development of sugar-nucleotide mimics, and illustrate the considerable potential of the squarylamide group as a fragment for inhibitor design.

Introduction

Sugar-nucleotides[1] such as GDP-mannose (Fig. 1), GDP-fucose and UDP-glucose are important biomolecules with a central role in carbohydrate and glycoconjugate biosynthesis, metabolism and cell signalling.[1] In both prokaryotes and eukaryotes, sugar-nucleotides serve as donor substrates for Leloir-type glycosyltransferases [2,3] and other glycoprocessing enzymes. These enzyme classes have been identified as promising drug targets in various therapeutic areas, including infection,[4,5] inflammation,[6,7] and cancer.[7] Individual sugar-nucleotides also act as agonists at the human $P2Y_{14}$ receptor which has an important role in immune function.[8] Structural analogues and mimics of naturally occuring sugar-nucleotide are therefore of significant interest as candidate molecules for enzyme inhibitors, receptor ligands and chemical tools in medicinal chemistry and chemical biology.

Structurally, sugar-nucleotides (exemplified by GDP-mannose, Fig. 1) are composed of a sugar, or sugar derivative, and a nucleotide fragment. In mammalian cells, nine different sugar-nucleotides have been identified, but this number is much larger in other organisms.[1] In many cases the diphosphate linkage is essential for the interaction of the sugar-nucleotide with its target protein and thus for its biological activity. However, the diphosphate

[a]*School of Pharmacy, University of East Anglia, Norwich, UK NR4 7TJ. E-mail: g.wagner@uea.ac.uk; Fax: +44 (0)1603 592003; Tel: +44 (0)1603 593889*
[b]*Centre for Biomolecular Sciences, The North Haugh, The University, St. Andrews, KY16 9ST, Scotland*
[c]*Department of Computational & Systems Biology, John Innes Centre, Norwich, UK NR4 7UH*

† Electronic supplementary information (ESI) available: ^{1}H-NMR spectra for compounds **3**, **4**, **5a-g** and **6a-g**, ^{1}H-NMR titration curves for **5c** and **5g**, and ^{1}H-NMR spectra for the titration of **5g** with $MgCl_2$. See DOI: 10.1039/c004165c

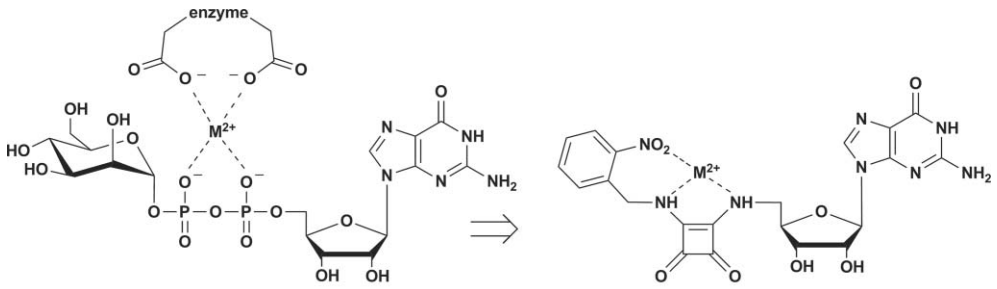

Fig. 1 Molecular structures of GDP-mannose (left) and of a representative squarylamide targeted in this study. Both the diphosphate group in GDP-mannose and the squaric acid moiety in the target squaryldiamides can coordinate to a divalent metal.

group also contributes to the limited stability and low membrane permeability of sugar-nucleotides, unfavourable properties which complicate their use as biological tools and therapeutic agents.[9] In order to develop sugar-nucleotide mimics with improved biological activity, chemical stability and membrane permeability, many efforts have therefore been directed at the identification of uncharged, chemically stable surrogates for the diphosphate linkage in sugar-nucleotides.[10,11] Functional groups that have been examined as potential diphosphate bioisosteres include phosphonates,[12–17] malonates,[18] malonodiamides,[19] tartrates,[18] vicinal alcohols,[20,21] monosaccharides,[18,22] amides,[23] sulfonamides,[23] and sulfamates.[24,25] However, despite these considerable efforts no generally applicable diphosphate bioisostere has so far been identified.

Leloir-type glycosyltransferases catalyse the transfer of a sugar (derivative) from the sugar-nucleotide donor to a suitable acceptor substrate.[2,3] In many cases, the diphosphate group of the donor sugar-nucleotide is critically involved in orienting the donor substrate in the correct, bioactive conformation, prior to the transfer reaction.[2,3] Glycosyltransferases of the GT-A family, one of two major glycosyltransferase fold families, require the presence of a divalent metal cation (typically Mn^{2+} or Mg^{2+}) in the active site for full catalytic activity.[2,3] The catalytic metal mediates sugar-nucleotide binding at the enzyme through simultaneous interaction with the aspartate residue(s) of the so called DXD motif characteristic for glycosyltransferases of the GT-A family and the diphosphate group of the sugar-nucleotide (Fig. 1).[2,3] Because of the importance of the sugar-nucleotide–metal interaction for ligand binding in GT-A glycosyltransferases, the capacity to coordinate to a divalent metal cation is an important design criterion in the development of sugar-nucleotide mimics as potential glycosyltransferase inhibitors. Interestingly, while for many of the previously published sugar-nucleotide mimics such a capacity for coordination to a divalent metal has been postulated, this has rarely been proven experimentally.

Recently, the squaric acid group has been reported as an uncharged mimic of the phosphate group in mono- and oligonucleotides.[26,27] However, the use of the squaric acid motif as a mimic for the diphosphate linkage in sugar-nucleotides has not previously been explored. To investigate this possibility, we have rationally designed a novel class of sugar-nucleotide mimics based on a squaric acid core as potential glycosyltransferase inhibitors (Fig. 1). Herein, we describe the design and synthesis of a series of novel squaryldiamides as potential mimics of GDP-sugars such as GDP-mannose, the donor substrate of Leloir-type mannosyltransferases. Importantly, we have also carried out NMR studies to determine experimentally the capacity of these novel squaryldiamides to coordinate to Mg^{2+}, an important prerequisite for binding at GT-A glycosyltransferases. To assess their biological activity, we have evaluated these novel GDP-sugar mimics as potential inhibitors of the GDP-mannose-dependent mannosyltransferase dolichol-phosphate mannose synthase (DPMS) from *Trypanosoma brucei*, a validated target for the development of novel *anti*-trypanosomal agents.[28,29] The squarylamide derivatives described herein are, to the best of our knowledge, the first examples for GDP-sugar mimics based on the squaric acid motif, and the main findings from this study may also have implications for the design of inhibitors for other metal-dependent glycosyltransferases.

Target design

The design of the GDP-sugar mimics targeted in this study was informed by the following considerations (Fig. 1): Because of its important contribution to binding, we decided to retain the guanosine part of GDP-mannose. The diphosphate linkage was to be replaced with a squaryldiamide group, which we expected to coordinate to the catalytic metal in the DPMS active site. Furthermore, we speculated that a suitable second substituent at the cyclobutene-1,2-dione core, *e.g.* a benzylamine substituent with a polar group at the *ortho* position (*cf.* **5c**, Fig. 1), might contribute to the interaction between inhibitor and metal through the formation of a chelate complex.

Before embarking on the synthesis of the target squaryldiamides, we wanted to assess whether the GDP-mannose binding site of a Leloir mannosyltransferase could accommodate these potential donor substrate mimics. We therefore carried out molecular docking studies with the target squaryldiamides and a representative mannosyltransferase, the fungal enzyme Kre2p.[30] Kre2p is one of only two GDP-mannose-dependent mannosyltransferases whose structures had been solved at the outset of this project.[30,31] Like *T. brucei* DPMS, for which no crystal structural is presently available, Kre2p requires a Mn^{2+} cofactor for catalytic activity.[30] The structure of Kre2p in complex with GDP, released as a by-product during the mannosyltransferase reaction, shows the nucleoside diphosphate bound to the donor binding site mostly by van der Waals and stacking interactions as well as key hydrogen bonds between and Asp161 and N1 and N2 of the guanine base.[30] In the binary Kre2p/GDP complex, Mn^{2+} forms important interactions with the α and β phosphates of GDP and Oε2 of Glu247.[30] Kre2p belongs to the GT-A fold family of glycosyltransferases. Structural comparison with other GT-A enzymes suggests that Glu247, Pro248 and Asp249 correspond to the so-called DXD motif, which is required in GT-A glycosyltransferases for the coordination of the divalent metal cofactor.[30] However, in the case of Kre2p, only Glu247, the first residue of the putative DXD motif, interacts directly with the Mn^{2+} ion.

Molecular docking studies with squaryldiamides **5a–g** indicated that these novel GDP-sugar mimics can bind to the Kre2p sugar-nucleotide binding site in a similar orientation as GDP. Docking results for the representative squarylamide **5c** show the guanine base buried deep in the donor binding site and forming a hydrogen bond with Asp161 (Fig. 2). Both the squaryldiamide core and the 2-nitrobenzyl substituent of **5c** are in close proximity to the Mn^{2+} ion, which interacts with Glu247 in a similar fashion as in the Kre2p/GDP complex. Squaryldiamide **5c** coordinates to the metal cofactor *via* the oxygen atoms of the nitro group (distances: 1.6 Å and 1.7 Å) and the two squaryldiamide nitrogen atoms (distances: 3.9 Å and 4.1 Å), forming a chelate complex. We concluded from these molecular docking results that the target squaryldiamides can indeed adopt a similar geometry as GDP/GDP-mannose and coordinate efficiently to the divalent metal co-factor in the donor binding site of a mannosyltransferase. We therefore set out to test these hypotheses experimentally

Chemistry

Asymmetrical squaryldiamides can be prepared by sequential reaction of a squaric acid dialkylester with two different amines.[26,27]

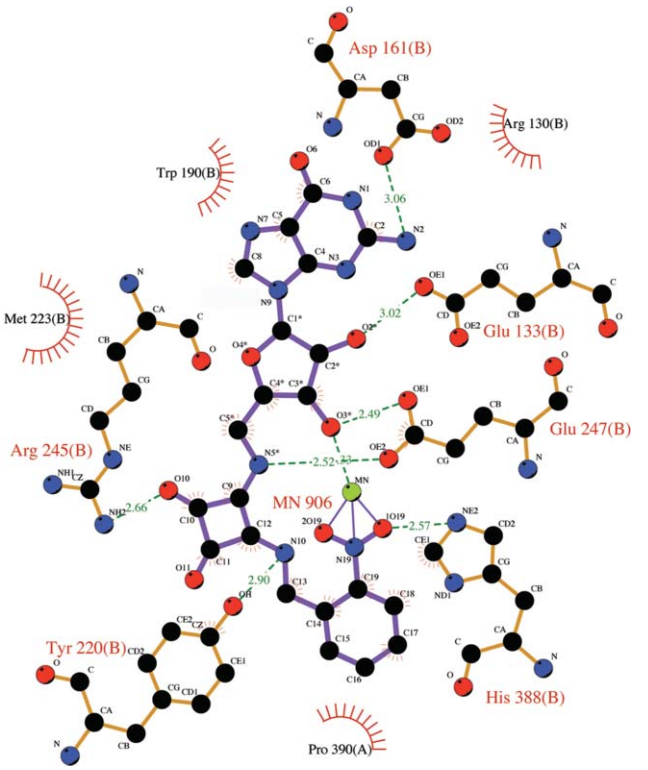

Fig. 2 Ligand-enzyme interactions of **5c** in domain B of Kre2p as predicted by molecular docking. Key: H-bonds – green, hydrophobic contacts – red, ligand bonds – purple, non-ligand bonds – brown. Picture created with LigPlot [47]

Initially, we planned to install the aminoguanosine fragment, which is present in all analogues, first, and the benzylamino substituent, which is variable, second (Fig. 3, Strategy A). This approach is advantageous in that it allows structural diversification at the last step of the synthesis. Alternatively, the two different substituents can also be introduced in the reverse order (Fig. 3, Strategy B). For both synthetic pathways, 5′-deoxy-5′-aminoguanosine **3** was required as a key synthetic building block. **3** was prepared in three steps from guanosine in 45% overall yield *via* an adaptation of Dean's procedure (Scheme 1).[32] This reaction sequence involved the synthesis of 5′-deoxy-5′-iodoguanosine **1** from guanosine *via* the selective substitution of the primary alcohol with an iodo group, the conversion of **1** into 5′-deoxy-

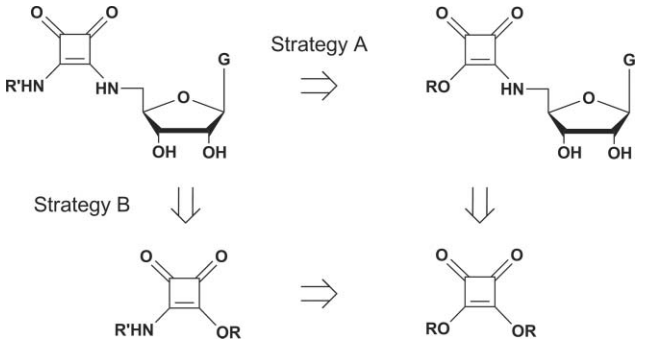

Fig. 3 General synthetic strategy for target squaryldiamides (G: guanine; R: ethyl or methyl; R′: various substituents).

5′-azidoguanosine **2**, and the PPh_3-mediated reduction of azide **2** to amine **3**.

In the next step, strategy A (Fig. 3) required the preparation of squarylmonoamide **4** from aminoguanosine **3** and a suitable dialkylsquarate. Initially, we were concerned that this reaction might be complicated by the formation of side products (*e.g.* symmetrical or mixed squaryldiamides), potentially necessitating the protection of the amino group in position 2 of the nucleobase. Much to our delight we found that at room temperature in DMF, the base-catalyzed reaction of diethylsquarate with **3** proceeds exclusively at the aliphatic amino group in position 5′. Despite a prolonged reaction time of 92 h, no diamides were detected, and no reaction was observed with the amino group in position 2. In the ^{1}H NMR spectrum of **4**, the broad, exchangeable signal at $\delta =$ 6.47 ppm, corresponding to the free amino group, confirms that no reaction had occurred between this group and diethylsquarate. This lack of reactivity of the amino group in position 2 is perhaps not surprising, given the electron-withdrawing effect of the purine ring system, which may contribute to the reduced nucleophilicity of the amino group.

Interestingly, the ^{1}H NMR spectrum of **4** showed two sets of signals for the squarylamide proton (two triplets at, respectively, $\delta = 8.74$ and 8.89 ppm), for both protons in position 5′ of the ribose, and for the protons of the ethyl group. The two sets of signals can be attributed to the presence of **4** in two stable rotameric forms, *syn* and *anti* (Fig. 4). In the *syn* conformation, the squarylamide proton is facing towards the adjacent carbonyl group, and in the *anti* conformation away from it. The existence

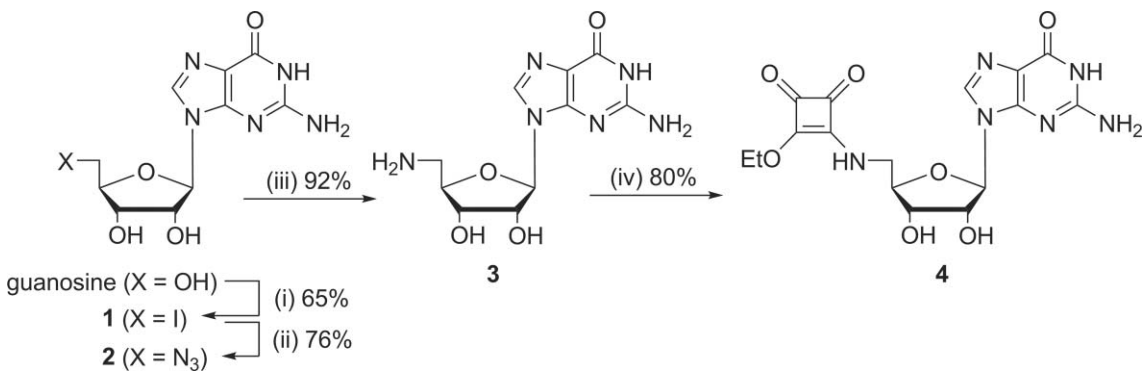

Scheme 1 Synthesis of key intermediates **3** and **4**. Reagents and conditions: (i) I_2, PPh_3, imidazole, DMF, rt, 4 h, 65%; (ii) NaN_3, DMF, 90 °C, 22 h, 76%; (iii) (a) PPh_3, pyridine, rt, 5h; (b) NH_3(aq), rt, 39 h, 92%; (iv) diethylsquarate, DIPEA, DMF, rt, 92 h, 80%.

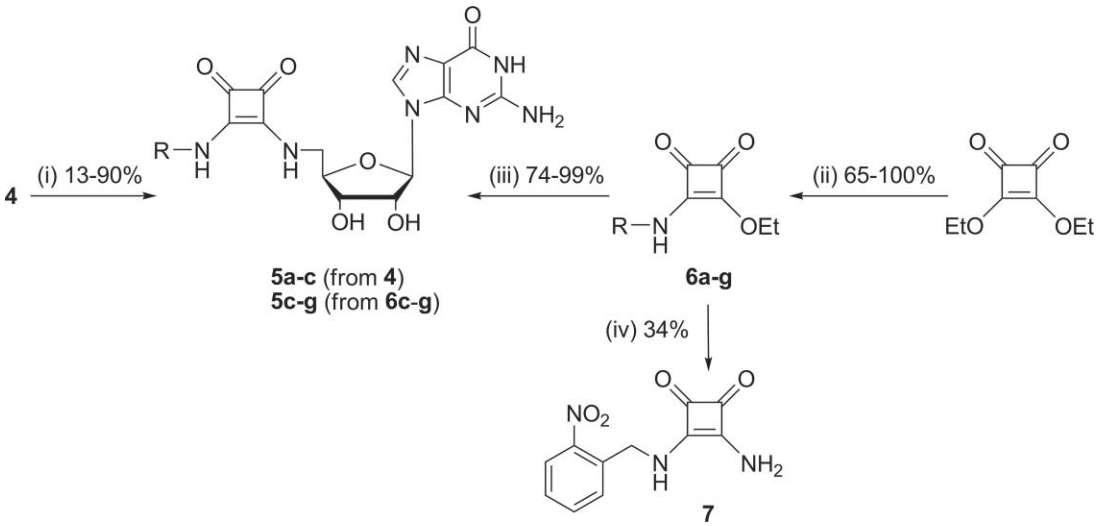

Scheme 2 Synthesis of target squaryldiamides **5**. Reagents and conditions: (i) R-NH_2, DIPEA, DMF, rt, 1–7 days; (ii) R-NH_2, DIPEA, EtOH or MeOH, rt, 2–16 h; (iii) **3**, DIPEA, DMF, rt, 5–7 days; (iv) aq. NH_3 (35%), MeOH, 50 °C, 2 days. *Substituents R*: (a) n-butyl; (b) benzyl; (c) 2-NO_2 benzyl; (d) 3-NO_2 benzyl; (e) 4-NO_2 benzyl; (f) carboxypropyl; (g) 2-CO_2H benzyl.

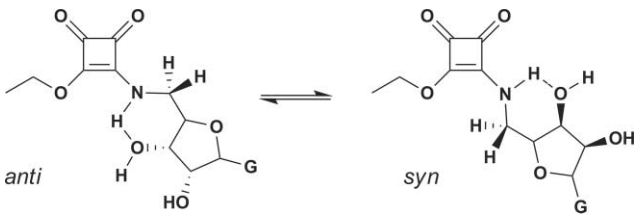

Fig. 4 Different rotamers of squarylamide **4**.

of stable rotamers has previously been described for other squarylmonoamides.[33,34] The interconversion of these rotamers can be slow due to the delocalisation of the nitrogen lone pair electrons with the cyclobutene-1,2-dione system and, as a result, the restricted rotation about the squarylamide carbon-nitrogen bond. Individual rotamers can also be stabilised by intramolecular hydrogen bonding.[33,34] The ^{1}H NMR spectrum of **4** suggests that in solution, this squarylamide exists as a 1 : 1 mixture of the *syn* and *anti* rotamer. Only one set of signals is observed, however, for the ribose protons 1′–4′ of **4**, which indicates a similar orientation and conformation of the ribose ring in both rotamers.

In order to obtain the target squaryldiamides **5**, squarylmonoamide **4** was reacted with different amines (Scheme 2). All amines required for the synthesis of the target squaryldiamides were commercially available, with the exception of 2-aminomethylbenzoic acid, which was synthesised in two steps according to Sun's procedure.[35] The reaction with squarylmonoamide **4** proceeded only sluggishly (1–2 days at room temperature) with both benzylamine and n-butylamine (Scheme 2, **5a** and **5b**), and even more so with 2-nitrobenzylamine (**5c**; 7 days at room temperature, followed by 4 days at 60 °C). The extremely prolonged reaction time and the low isolated yield for **5c** prompted us to explore an alternative synthetic route for the preparation of further analogues.

To our satisfaction, we found that reversing the last two reaction steps of our general synthesis offered a more practical approach (Fig. 3, Strategy B). Thus, squarylmonoamides **6a–g** were prepared in mostly excellent yields and with comparatively short reaction times from diethylsquarate and the respective primary amine (Scheme 2). In the subsequent step, the target squaryldiamides **5c–g** were obtained in good to excellent yields from monoamides **6c–g** and aminoguanosine **3**. While these reactions proceeded not significantly faster than the reaction of **4** with a primary amine, they yielded cleaner reaction products, thus facilitating purification. Finally, squarylmonoamide **6c** was also reacted with aqueous ammonia to give the corrsponding squaryldiamide **7**, which was required as a model compound for the NMR titration experiments that were carried out next.

Coordination to Mg^{2+}

In a series of squaryldiamide oligonucleotide mimics, a pronounced downfield shift had previously been observed for the ^{1}H NMR signals of the squarylamide protons upon addition of $MgCl_2$.[26] This downfield shift had been attributed to the coordination of the divalent metal ion to the squarylamide group and a subsequent increase in acidity of the amide protons.[26] We reasoned that this effect could be used as a diagnostic marker to assess experimentally the predicted ability of the novel squarylamides **5** to coordinate to divalent metal ions. To test this hypothesis, we carried out comprehensive ^{1}H NMR titration experiments with three representative target compounds **5b**, **5c** and **5g** and $MgCl_2$ in DMF-d_7.

In the case of all three squaryldiamides **5b**, **5c** and **5g**, upon addition of $MgCl_2$ a significant downfield shift was observed for the signals corresponding to the two squarylamide protons, as well as for those corresponding to the exchangeable NH and NH_2 protons on the guanine base (Fig. 5 and ESI†). The representative titration curve for **5b** is shown in Fig. 5, with the chemical shift values plotted against equivalents of $MgCl_2$. Initially, the chemical shift changes are very pronounced for all four signals, before a plateau is reached at approximately two equivalents of $MgCl_2$. This suggests a 1 : 2 stoichiometry for the **5b**–Mg^{2+} complex, with one equivalent of Mg^{2+} coordinating to the squaryldiamide group,

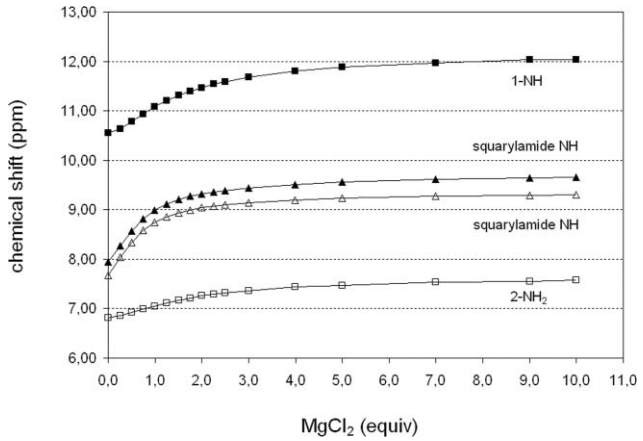

Fig. 5 NMR titration experiment with squarylamide **5b**.

and a second equivalent in complex with the pyrimidine fragment of the guanine base. The curves for the two squarylamide proton signals show a particularly steep initial gradient, up to the addition of approximately one equivalent of $MgCl_2$, while the gradient for the curves of the guanine NH and NH_2 signals is more shallow. The steeper curve for the squaryldiamide protons may suggest that coordination of the first equivalent of Mg^{2+} occurs preferentially at this position. This interpretation is supported by the equivalence points determined for each titration. Extrapolation of the steep initial and the shallow terminal sections of each curve results in intersections, corresponding to the respective equivalence point, at one equivalent of $MgCl_2$ for the squaryldiamide protons, and at two equivalents of $MgCl_2$ for the guanine protons.

To better understand the coordination behaviour of the squarylamide group, we carried out further titration experiments with squarylmonoamide **6c** and model squaryldiamide **7** (Fig. 6). We anticipated that the formal removal of the guanosine fragment in these two analogues would simplify the analysis of the titration results. Also, information about the precise site at the cyclobutene-1,2-dione core that is involved in coordination of the metal ion may be obtained from direct comparison of **6c** and **7**. Previously, Sato *et al.* have suggested for a model thymidine-based squaryldiamide that Mg^{2+} coordinates to the oxygen rather than the nitrogen atoms of the squaryldiamide group.[26] In this case, **6c** and **7** would be expected to display very similar metal coordination behaviour.

Although the initial gradient is steeper, the titration curves for the squarylamide protons in **7** correspond to those observed for the squarylamide signals in **5b**, suggesting a similar coordination behaviour at the squarylamide group (Fig. 6a). In contrast to the results for **7**, titration of squarylmonoamide **6c** with up to 10 equivalents of $MgCl_2$ did not produce a stable endpoint for the downfield shift of the amide proton signal, and no equivalence point could be determined for this compound (Fig. 6b; the two curves are for the amide proton of the two rotamers). The different titration results for squaryldiamide **7** and monoamide **6c** suggest that efficient coordination of Mg^{2+} to the cyclobutene-1,2-dione core requires the presence of *two* amide nitrogens, indicating that the amide nitrogens rather than the two oxo groups are directly involved in formation of the complex with the metal. Monoamide **6c** may still be surrounded by several equivalents of $MgCl_2$, as evidenced by the downfield shift of the squarylamide proton signals, but direct coordination to the metal appears to be relatively

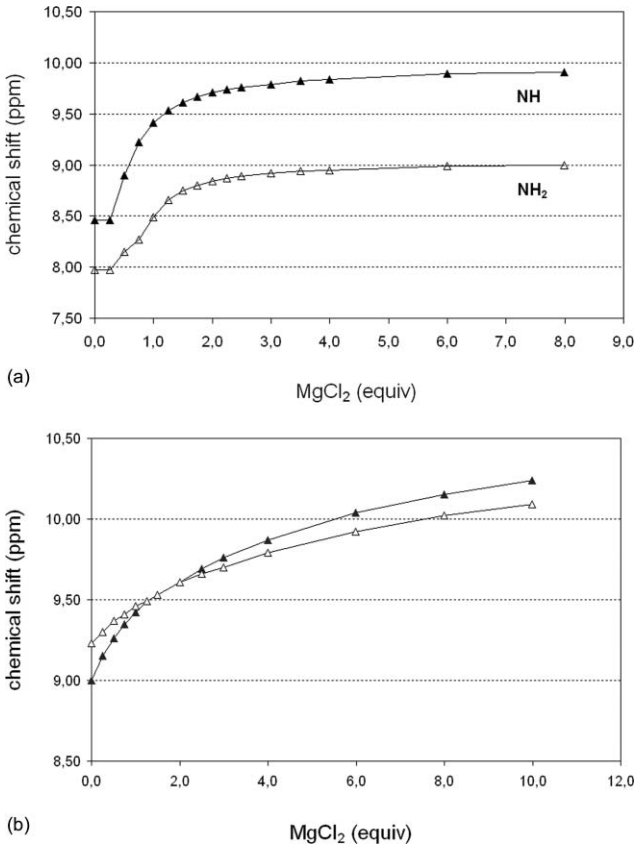

Fig. 6 NMR titration experiment with (a) squaryldiamide **7**, and (b) squarylmonoamide **6c**.

weak. Importantly, coordination of the metal at the squarylamide nitrogens also allows the ligand to adopt an orientation favourable for binding to protein, as predicted by the results from molecular docking (Fig. 2).

In summary, the results from the NMR titration experiments with the novel squarylamides **5b**, **5c**, **5g**, **6c** and **7** suggested to us that the diamides, if perhaps not the monoamides, coordinate readily to a divalent metal such as Mg^{2+}. With this feature, the squaryldiamides meet, as expected, an important prerequisite for effective diphosphate mimicry. Therefore, we next investigated if the capacity for the coordination of divalent metals would translate into biological activity towards a representative GDP-mannose-dependent mannosyltransferase.

Biological results

The trypanosomal parasite *Trypanosoma brucei* is the causative agent of African sleeping sickness (African trypanosomiasis), which puts more than 60 million people at risk in sub-Saharan Africa and led to 48,000 deaths in 2002 alone.[36] Current treatments for African trypanosomiasis are limited and problematic due to toxicity, expense, administration routes and resistance, thus new therapeutic approaches are urgently required. *T. brucei* has a cell-surface protective coat of variant surface glycoproteins (VSG) which the parasite uses to evade the immune system of the host. The biosynthesis of glycosylphosphatidylinositol (GPI) anchors, which link the VSG coat to the parasite membrane, has been validated genetically and chemically as a therapeutic target.[28,37,38]

Table 1 Biological activity of squarylamides and reference compounds

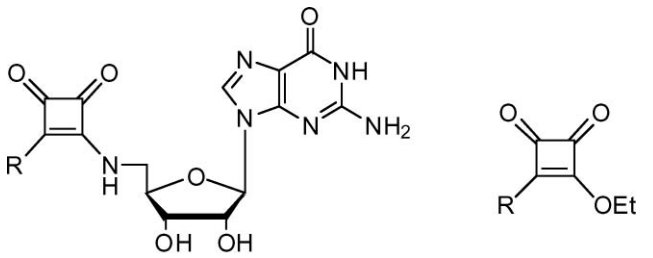

4, 5a-g **6b-c**

Compound	R	Residual DPMS activity (%)[a]	ED_{50}/mM[b]
control	na[c]	100 ± 3.0	na
GDP-mannose[d]	na	1.5 ± 0.2	nd[e]
GTP[d]	na	27.3 ± 3.8	nd
GDP[d]	na	8.5 ± 1.8[f]	nd
GMP[d]	na	78.2 ± 2.3	nd
guanosine	na	97.4 ± 4.5	nd
4	ethoxy	87.1 ± 0.2	1.1 ± 0.2
5a	n-butylamino	81.3 ± 0.3	1.0 ± 0.1
5b	benzylamino	78.0 ± 2.0	0.725 ± 0.2
5c	2-nitrobenzylamino	84.1 ± 5.2	>1.5
5d	3-nitrobenzylamino	69.6 ± 2.1	low solubility
5e	4-nitrobenzylamino	65.1 ± 3.0	low solubility
5f	carboxypropylamino	91.9 ± 5.6	0.985 ± 0.2
5g	2-carboxybenzylamino	64.0 ± 1.0	1.0 ± 0.2
6b	benzylamino	97.9 ± 0.7	>1.5
6c	2-nitrobenzylamino	104.4 ± 6.3	>1.5

[a] In the presence of 1 mM inhibitor, unless stated otherwise; values are means ± SD of 3 separate determinations counted twice. [b] Values are means ± SD of 4 separate determinations. [c] Not applicable. [d] At 0.1 mM concentration. [e] Not determined. [f] $IC_{50} = 32 \pm 4$ μM.

The mannosyltransferase dolichol-phosphate mannose synthase (DPMS) is a Mg^{2+}-dependent enzyme which catalyses the formation of dolichol-phosphate-mannose (Dol-*P*-Man) from GDP-mannose and dolichol-phosphate. In all eukaryotes, Dol-*P*-Man is the essential mannose donor for all three mannosyltransferases involved in GPI anchor biosynthesis, and for the last four mannosyltransferases involved in *N*-glycosylation. Because of its central role in GPI biosynthesis and *N*-glycosylation of VSG, DPMS represents a promising new target for the development of novel *anti*-trypanosomal agents.[39]

In order to assess the DPMS-inhibitory activity of the novel squaryldiamides, full-length *T. brucei* DPMS was recombinantly expressed in *E. coli*, and DPMS-containing membranes were used to catalyse the formation of didehydrofarnesol-phosphate[^{3}H]mannose ([^{3}H]-DFPM) from GDP-[^{3}H]mannose and didehydrofarnesol-phosphate in the presence or absence of potential inhibitor. The residual DPMS activity in the presence of inhibitor was determined from the amount of [^{3}H]-DFPM formed, relative to the amount of [^{3}H]-DFPM formed in the non-inhibited reaction (Table 1). For direct comparison, inhibition experiments were also carried out with non-labelled GDP-mannose, GDP, which is a by-product of the DPMS reaction and known feedback inhibitor of DPMS,[29] GTP, GMP and guanosine. Under these conditions, GDP-mannose, GDP and, to a lesser degree, GTP and GMP, but not guanosine, significantly reduced the DPMS-catalysed formation of [^{3}H]-DFPM. For GDP, we determined an IC_{50} value of 32 μM. The significant difference in activity between guanosine on the one hand, and the guanine nucleotides and GDP-mannose on the other illustrates the importance of the phosphate groups for ligand binding, presumably through coordination of the active site metal. Somewhat disappointingly, however, most squarylamides showed only low to moderate inhibition of DPMS activity at a concentration of 1 mM. Thus, the experimentally demonstrated capacity of analogues **5b**, **5c** and **5g** to coordinate to Mg^{2+} did translate into DPMS inhibitory activity *in vitro*, but to a lesser degree than expected. The most potent DPMS inhibitor in this series is the 2-carboxybenzylamino derivative **5g**, which also coordinates effectively to Mg^{2+}. Interestingly, in the nitrobenzyl series (**5c–e**), those analogues with the nitro group in the *meta* (**5d**) or *para* position (**5e**) were slightly more potent than 2-nitrobenzylamino derivative **5c**. This suggests that the contribution of a polar substituent in the *ortho* position to stabilisation of the ligand-metal complex may be less relevant, at least *in vitro*, than predicted by the Mg^{2+} titration experiments. Analogues lacking the guanosine fragment (**6b**, **6c**) are inactive, which was expected, as this motif is known to be important for biological activity.

We also evaluated squaryldiamide **5c** for its inhibitory activity against *T.brucei* GDP-Man pyrophosphorylase (GDP-Man PP). GDP-Man catalyses the formation of GDP-Man from GTP and mannose-1-phosphate and has been validated as a therapeutic target.[38] Interestingly, **5c** acted as an inhibitor of GDP-Man PP with an IC_{50} of 0.7 mM, suggesting that this squaryldiamide may be able to mimic not only GDP-mannose, but also GTP binding. Selected squarylamides were also tested for trypanocidal activity against the bloodstream form of *T. brucei* in the Alamar Blue cytotoxicity assay.[40] Several analogues in this series showed activity against live trypanosomes with ED_{50} values of, or below, 1 mM (Table 1). The strongest effect *in vivo* was observed for benzylamino derivative **5b**, while 2-carboxybenzylamino derivative **5g**, which showed relatively potent DPMS inhibition, had comparatively modest trypanocidal activity. The limited trypanocidal activity of **5g** may be due to its unfavourable physicochemical properties, which may compromise its penetration through the cell membrane of the parasite.

Discussion and conclusion

In light of their experimentally demonstrated ability to coordinate to Mg^2, the relatively limited DPMS inhibitory activity of the novel squarylamides was surprising. It can be speculated that this may be due to the unfavourable conformational preferences of our novel squarylamides. 2D NMR spectra from NOESY and ROESY experiments with **4** show interactions between the squarylamide proton and protons in position 5′, 4′ and 3′ of the ribose (Fig. 7). The close proximity of the amide proton and these protons suggests that both rotamers adopt a "bicyclic" conformation, possibly stabilised by an internal hydrogen bond between the amide proton and the 3′-hydroxyl group (Fig. 4). An important difference between both rotamers is the orientation of the guanosine part relative to the cyclobutene-1,2-dione ring. Sugar-nucleotides frequently adopt an extended conformation, both in solution[41] and bound to protein.[42] It appears that in the case of our novel squarylamides, only the *anti* rotamer can act as an effective mimic of this extended sugar-nucleotide conformation.

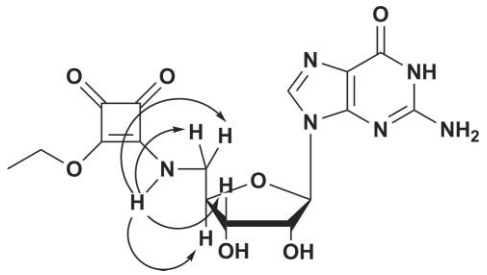

Fig. 7 NOE interactions observed for both rotamers of squaryl-monoamide **4**.

At the same time, the conversion of the complete population of a given squarylamide into the favourable *anti* rotamer may be associated with a prohibitively high energy barrier, resulting from restricted rotation about the squarylamide bond.

In summary, we have developed a series of squaryldiamides as novel and rationally designed sugar-nucleotide mimics. A key design criteria was the capacity of the squaric acid fragment to coordinate to divalent metal ions. Importantly, we could demonstrate experimentally that the new squaryldiamides coordinate readily to Mg^{2+}, thus mimicking an essential property of the diphosphate linkage in sugar-nucleotides. The squaryldiamides described herein therefore represent one of the first examples for a sugar-nucleotide mimic whose capacity for metal coordination has been experimentally demonstrated. Several analogues from this series possess some biological activity against recombinant DPMS, and the most potent squaryldiamide **5b** was effective against the bloodstream form of *T. brucei* with an ED_{50} of 700 μM. Conformational studies suggest that the generally only modest bioactivity of these squarylamides may be due to their unfavourable conformational preferences. Taken together, our results suggest that squaryldiamides are a promising template for further development of sugar-nucleotide mimics and novel glycosyltransferase inhibitors. Our findings illustrate the considerable potential of the squarylamide group as a fragment for inhibitor design. Future studies in this area will need to give due consideration to conformational aspects of this exciting structural class.

Experimental section

General

All reagents were obtained commercially and used without further purification unless stated otherwise. TLC was carried out on commercially available TLC aluminium sheets and spots were visualised under UV at 254 nm. For preparative column chromatography silica 60 (particle size 0.063–0.2 mm) was used. Solvents are stated in portions of volume. ^{1}H NMR and ^{13}C NMR spectra were recorded at, respectively, 399.918 MHz (^{1}H) and 75.456 MHz (^{13}C) on a Varian VXR 400 S spectrometer. Chemical shifts δ are measured from the deuterium lock peak of the solvent and are recorded in ppm. Coupling constants J are given in Hz and signal multiplicities are reported as follows: s = singlet, d = duplet, dd = duplet of duplets, t = triplet, q = quartet, m = multiplet and br = broad. Melting points were measured on a capillary melting point apparatus and are not corrected. Mass spectra were recorded at the EPSRC National Mass Spectrometry Service Centre, University of Wales, Swansea.

2-Amino-9-((2*R*,3*R*,4*S*,5*S*)-3,4-dihydroxy-5-(iodomethyl)-tetrahydrofuran-2-yl)-1*H*-purin-6(9*H*)-one (1).[32] To a suspension of guanosine (10.02 g, 35.38 mmol), triphenylphosphine (30.62 g, 116.7 mmol) and imidazole (15.9 g, 243.3 mmol) in anhydrous DMF (135 mL), iodine (28.47 g, 112.2 mmol) was added in portions, over a period of five minutes, while stirring vigorously. The orange solution was cooled to room temperature and stirred for 4 h. The reaction mixture was poured into a stirred mixture of DCM (1300 mL) and water (400 mL). A white precipitate formed at the interface of the two layers. The precipitate was filtered off, washed with DCM (100 mL) and dried at room temperature overnight to give **1** as a white powder in 65% yield (9.02 g, 22.9 mmol): R_f 0.37 (DCM–MeOH 7 : 3); mp 178 °C (decomposition); δ_H (400 MHz, DMSO-d_6) 3.41 (dd, 1H, J = 10.3 Hz, 10.6 Hz, H-5′), 3.55 (dd, 1H, J = 10.3 Hz, 10.6 Hz, H-5′), 3.93 (m, 1H, J = 5.9 Hz, 6.2 Hz, H-4′), 4.06 (br, 1H, H-3′), 4.63 (br, 1H, H-2′), 5.40 (br, 1H, 3′-OH), 5.56 (br, 1H, 2′-OH), 5.70 (d, 1H, J = 6.2 Hz, H-1′), 6.51 (s, 2H, 2-NH_2), 7.92 (s, 1H, H-8), 10.68 (s, 1H, H-1).

2-Amino-9-((2*R*,3*R*,4*S*,5*S*)-3,4-dihydroxy-5-(azidomethyl)-tetrahydrofuran-2-yl)-1*H*-purin-6(9*H*)-one (2).[32] A solution of **1** (7.45 g, 18.9 mmol) and sodium azide (1.70 g, 26.1 mmol) was stirred in anhydrous DMF (50 mL) at 90 °C for 22 h. The solvent was removed *in vacuo*. The solid residue was triturated with water (100 mL), filtered off, washed with water (2 × 50 mL), EtOH (25 mL) and diethylether (25 mL), and dried at room temperature to give **2** as a dark yellow powder in 76% yield (4.45 g, 14.4 mmol): R_f 0.35 (DCM–MeOH 7 : 3); mp 241 °C (decomposition); δ_H (400 MHz, DMSO-d_6) 3.51 (dd, 1H, J = 12.8 Hz, 13.2 Hz, H-5′), 3.67 (dd, 1H, J = 12.8 Hz, 13.2 Hz, H-5′), 3.98 (q, 1H, J = 3.3 Hz, H-4′), 4.06 (t, 1H, J = 3.7 Hz, 4.0 Hz, H-3′), 4.58 (t, 1H, J = 5.1 Hz, H-2′), 5.35 (br, 1H, 3′-OH), 5.57 (br, 1H, 2′-OH), 5.72 (d, 1H, J = 5.5 Hz, H-1′), 6.55 (s, 2H, 2-NH_2), 7.91 (s, 1H, H-8), 10.72 (br, 1H, H-1).

2-Amino-9-((2*R*,3*R*,4*S*,5*S*)-3,4-dihydroxy-5-(aminomethyl)-tetrahydrofuran-2-yl)-1*H*-purin-6(9*H*)-one (3).[32] Triphenylphosphine (1.71 g, 6.52 mmol) was added to a solution of **2** (1.00 g, 3.24 mmol) in anhydrous pyridine (20 ml). The reaction was stirred for 5 h at room temperature. Water (20 mL) and aqueous ammonia (35%, 6.5 mL) were added, and the reaction was stirred for another 39 h. The solvents were removed *in vacuo*. The residue was triturated with EtOAc (85 mL) for 15 min, filtered off, and washed consecutively with EtOAc, cold EtOAc–MeOH (1 : 1) and water. The product was dried at 105 °C for two days to give **3** as a white powder in 92% yield (0.84 g, 2.98 mmol): mp 216 °C (decomposition); δ_H (400 MHz, DMSO-d_6) 2.70 (dd, 1H, J = 5.1 Hz, 13.6 Hz, H-5′), 2.78 (dd, 1H, J = 5.1 Hz, 13.6 Hz, H-5′), 3.35 (br, 2H, 5′-NH_2), 3.78 (m, 1H, H-4′), 4.07 (m, 1H, H-3′), 4.43 (dd, 1H, J = 3.3 Hz, 5.5 Hz, H-2′), 5.02 (br, 1H, 3′-OH), 5.38 (br, 1H, 2′-OH), 5.66 (d, 1H, J = 5.9 Hz, H-1′), 6.50 (s, 2H, 2-NH_2), 7.94 (s, 1H, H-8).

3-(((2*R*,3*S*,4*R*,5*R*)-5-(2-Amino-6-oxo-1*H*-purin-9(6*H*)-yl)-3,4-dihydroxytetrahydrofuran-2-yl)methylamino)-4-ethoxycyclobut-3-ene-1,2-dione (4). To a solution of **3** (401 mg, 1.42 mmol) in anhydrous DMF (35 mL), DIPEA (125 μL, 92.0 mg, 0.71 mmol) and 3,4-diethoxycyclobut-3-ene-1,2-dione (215 μL, 248 mg, 1.46 mmol) were added. The reaction was stirred for

92 h at room temperature. The solvent was removed *in vacuo*. The residue was sonicated with acetone for five minutes, filtered off, washed with acetone and dried at 105 °C overnight to give **4** as a light yellow powder in 80% yield (464 mg, 1.14 mmol): R_f 0.62 (DCM–MeOH–water 7 : 7 : 1); mp 196 °C (decomposition); δ_H (400 MHz, DMSO-d_6) 1.29 (t, 1.5H, J = 7.0 Hz, CH_3), 1.36 (t, 1.5H, J = 7.0 Hz, Et: CH_3), 3.46–3.65 (m, 1H, H-5′), 3.65–3.89 (m, 1H, H-5′), 3.93 (br, 1H, H-4′), 4.11 (br, 1H, H-3′), 4.45 (br, 1H, H-2′), 4.61 (m, 2H, Et: CH_2), 5.28 (br, 1H, 3′-OH), 5.53 (br, 1H, 2′-OH), 5.68 (d, 1H, J = 4.8 Hz, H-1′), 6.47 (d, 2H, J = 9.9 Hz, 2-NH_2), 7.83 (s, 1H, H-8), 8.74 (t, 0.5H, J = 5.1 Hz, 5′-NH), 8.89 (t, 0.5H, J = 4.4 Hz, 5′-NH), 10.67 (s, 1H, NH-1); δ_C (75 MHz, DMSO-d_6) 15.6 (Et: CH_3), 46.2 (C-5′), 69.3 (Et: CH_2), 72.7 (C-3′), 73.0 (C-2′), 83.2 (C-4′), 87.2 (C-1′), 117.3 (C-5), 136.5 (C-8), 151.5 (C-4), 153.8 (C-2), 157.1 (C-6), 174.6 (Sq: C-3), 177.4 (Sq: C-4), 182.7 (Sq: C-2), 190.1 (Sq: C-1). m/z (ESI) 406.1237 ($C_{16}H_{18}N_6O_7$ requires 406.1237).

Preparation of squaryldiamides 5a–c from squarylmonoamide 4

3-(((2*R*,3*S*,4*R*,5*R*)-5-(2-Amino-6-oxo-1*H*-purin-9(6*H*)-yl)-3,4-dihydroxytetrahydrofuran-2-yl)methylamino)-4-(butylamino)cyclobut-3-ene-1,2-dione (5a). To a solution of 4 (50.0 mg, 123 µmol) in anhydrous DMF (1 mL) were added first DIPEA (11.0 µL, 8.2 mg, 63.1 µmol), and then n-butylamine (13.5 µL, 10.0 mg, 137 µmol). The reaction mixture was stirred at room temperature for two days. The solvent was removed *in vacuo*, and the residue was sonicated with acetone for five minutes. The precipitate was filtered off, washed and dried at 105 °C overnight to give **5a** as a pale yellow powder in 79% yield (42.1 mg, 97.1 µmol): R_f 0.62 (DCM–MeOH–water 7 : 7 : 1); mp 238 °C (decomposition); δ_H (400 MHz, DMSO-d_6) 0.87 (t, 3H, J = 5.2 Hz, Bu: CH_3), 1.29 (m, 2H, Bu: C^3H_2), 1.47 (m, 2H, Bu: C^2H_2), 3.44 (m, 1H, H-5′), 3.49 (br, 2H, Bu: C^1H_2), 3.70 (m, 1H, H-5′), 3.95 (br, 1H, H-4′), 4.05 (br, 1H, H-3′), 4.52 (br, 1H, H-2′), 5.32 (br, 1H, 3′-OH), 5.54 (br, 1H, 2′-OH), 5.72 (d, 1H, J = 4.6 Hz, H-1′), 6.54 (br, 2H, 2-NH_2), 7.43 (br, 2H, Sq: NH), 7.89 (s, 1H, H-8), 10.74 (br, 1H, NH-1); δ_C (75 MHz, DMSO-d_6) 13.5 (Bu: CH_3), 19.1 (Bu: C^3H_2), 32.8 (Bu: C^2H_2), 42.9 (Bu: C^1H_2), 45.5 (C-5′), 70.8 (C-3′), 72.7 (C-2′), 83.6 (C-4′), 86.7 (C-1′), 116.9 (C-5), 136.1 (C-8), 151.4 (C-4), 153.6 (C-2), 156.9 (C-6), 167.9 (Sq: C-3), 168.2 (Sq: C-4), 175.9 (Sq: C-1), 182.5 (Sq: C-2). m/z (ESI) 433.1709 ($C_{18}H_{23}N_7O_6$ requires 433.1710).

3-(((2*R*,3*S*,4*R*,5*R*)-5-(2-Amino-6-oxo-1*H*-purin-9(6*H*)-yl)-3,4-dihydroxytetrahydrofuran-2-yl)methylamino)-4-(benzylamino)cyclobut-3-ene-1,2-dione (5b). To a solution of **4** (47.2 mg, 116 µmol) in anhydrous DMF (1.25 mL) were added first DIPEA (10.4 µL, 7.7 mg, 60 µmol), and then benzylamine (12.7 µL, 12.5 mg; 120 µmol). The reaction mixture was stirred overnight at room temperature. The solvent was removed *in vacuo* and the residue was sonicated with dichloromethane–hexane (2 : 1, 10 mL) for five minutes. The residue was filtered off, washed and dried at 105 °C overnight to give **5b** as a light brown powder in 90% yield (49.0 mg, 105 µmol): R_f 0.57 (DCM–MeOH–water 7 : 7 : 1); mp 211 °C (decomposition); δ_H (400 MHz, DMSO-d_6) 3.71 (m, 1H, H-5′), 3.94 (m, 1H, H-4′), 4.05 (br, 1H, H-3′), 4.51 (m, 1H, H-2′), 4.70 (br, 2H, Bn: CH_2), 5.31 (br, 1H, 3′-OH), 5.53 (d, 1H, J = 5.5 Hz, 2′-OH), 5.71 (d, 1H, J = 6.2 Hz, H-1′), 6.50 (br, 2H, 2-NH_2), 7.30 (t, 3H, J = 6.2 Hz, Ph: H-3, 4, 5), 7.37 (d, 2H, J = 7.0 Hz, Ph: H-2, 6), 7.43 (t, 1H, J = 6.2 Hz, Sq-NH), 7.80 (br, 1H, Sq-NH), 7.88 (s, 1H, H-8), 10.64 (br, 1H, NH-1); δ_C (75 MHz, DMSO-d_6) 45.5 (C-5′), 46.7 (Bn: CH_2), 70.8 (C-3′), 72.6 (C-2′), 83.4 (C-4′), 86.6 (C-1′), 117.0 (C-5), 127.4 (Ph: C-4), 127.5 (Ph: C-2, 6), 128.7 (Ph: C-3, 5), 136.0 (Ph: C-1), 138.9 (C-8), 151.4 (C-4), 153.8 (C-2), 156.8 (C-6), 167.7 (Sq: C-4), 167.8 (Sq: C-3), 182.8 (Sq: C-1), 189.1 (Sq: C-2). m/z (ESI) 467.1547 ($C_{21}H_{21}N_7O_6$ requires 467.1546).

3-(((2*R*,3*S*,4*R*,5*R*)-5-(2-Amino-6-oxo-1*H*-purin-9(6*H*)-yl)-3,4-dihydroxytetrahydrofuran-2-yl)methylamino)-4-(2-nitrobenzylamino)cyclobut-3-ene-1,2-dione (5c). To a solution of **4** (15.0 mg, 36.9 µmol) in anhydrous DMF (2 mL) were added first DIPEA (10.9 µL, 8.1 mg, 62.6 µmol), and then 2-nitrobenzylamine hydrochloride (8.3 mg, 44.0 µmol). The reaction mixture was stirred for seven days at room temperature, and then for four days at 60 °C. The solvent was removed *in vacuo*, and the residue was sonicated with acetone for five minutes. The precipitate was filtered off, washed and dried at 105 °C overnight to give **5c** as a brown powder in 13% yield (2.5 mg, 4.9 µmol): R_f 0.58 (DCM–MeOH–water 7 : 7 : 1); mp 240 °C (decomposition); δ_H (400 MHz, DMSO-d_6) 3.71 (m, 1H, H-5′), 3.94 (m, 1H, H-4′), 4.05 (br, 1H, H-3′), 4.51 (br, 1H, H-2′), 4.97 (d, 2H, J = 4.9 Hz, Bn: CH_2), 5.32 (br, 1H, 3′-OH), 5.54 (br, 1H, 2′-OH), 5.71 (d, 1H, J = 5.9 Hz, H-1′), 6.49 (br, 2H, 2-NH_2), 7.62 (m, 2H, Ph: H-4, 5), 7.71 (br, 1H, Sq-NH), 7.81 (d, 1H, J = 7.5 Hz, Ph: H-3), 7.89 (s, 1H, H-8), 7.91 (br, 1H, Sq-NH), 8.10 (d, 1H, J = 7.7 Hz, Ph: H-6), 10.66 (br, 1H, NH-1); δ_C (75 MHz, DMSO-d_6) 44.3 (C-5′), 45.6 (Bn: CH_2), 70.8 (C-3′), 72.7 (C-2′), 83.5 (C-4′), 86.8 (C-1′), 118.3 (C-5), 123.0 (Ph: C-2), 125.1 (Ph: C-6), 131.0 (Ph: C-5), 133.8 (Ph: C-3), 134.7 (Ph: C-4), 136.1 (C-8), 147.7 (Ph: C-1), 151.4 (C-4), 153.6 (C-2), 156.8 (C-6), 162.6 (Sq: C-4), 167.4 (Sq: C-3), 176.7 (Sq: C-1), 182.9 (Sq: C-2). m/z (ESI) 512.1403 ($C_{21}H_{20}N_8O_8$ requires 512.1404).

Preparation of squaryldiamides 5c–g from squarylmonoamides 6c–g

3-(((2*R*,3*S*,4*R*,5*R*)-5-(2-Amino-6-oxo-1*H*-purin-9(6*H*)-yl)-3,4-dihydroxytetrahydrofuran-2-yl)methylamino)-4-(2-nitrobenzylamino)cyclobut-3-ene-1,2-dione (5c). To a solution of **3** (10.1 mg, 35.8 µmol) in anhydrous DMF (2 mL) were added first DIPEA (6.3 µL, 4.7 mg, 36.2 µmol), and then **6c** (9.9 mg, 35.8 µmol). The reaction was stirred for five days at room temperature. The solvent was removed *in vacuo*, and the residue was purified by column chromatography. First, the column was eluted with DCM–MeOH (9 : 1) to remove unreacted **6c**, followed by elution with DCM–MeOH–water (7 : 7 : 1). Product-containing fractions were combined and the solvents were evaporated to give **5c** as a yellow powder in 92% yield (16.8 mg, 32.8 µmol).

3-(((2*R*,3*S*,4*R*,5*R*)-5-(2-Amino-6-oxo-1*H*-purin-9(6*H*)-yl)-3,4-dihydroxytetrahydrofuran-2-yl)methylamino)-4-(3-nitrobenzylamino)cyclobut-3-ene-1,2-dione (5d). To a solution of **3** (50.0 mg, 177 µmol) in anhydrous DMF (5 mL) were added first DIPEA (15.4 µL, 11.4 mg, 88.4 µmol), and then **6d** (49.0 mg, 177 µmol). The reaction was stirred for five days at room temperature. The solvent was removed *in vacuo*, and the residue was sonicated with acetone for five minutes. The precipitate was filtered off, washed with acetone and dried at 105 °C to give **5d** as a light yellow powder in 89% yield (80.9 mg, 158 µmol): R_f 0.49 (DCM–MeOH–water

7 : 7 : 1); mp 214 °C; δ_H (400 MHz, DMSO-d_6) 3.73 (m, 1H, H-5′), 3.96 (m, 1H, H-4′), 4.06 (d, 1H, J = 4.3 Hz, H-3′), 4.52 (m, 1H, H-2′), 4.84 (br, 2H, Bn: CH_2), 5.31 (br, 1H, 3′-OH), 5.54 (br, 1H, 2′-OH), 5.71 (d, 1H, J = 5.5 Hz, H-1′), 6.51 (br, 2H, 2-NH_2), 7.57 (m, 1H, Sq: NH), 7.68 (br, 1H, Ph: H-4), 7.89 (s, 1H, H-8), 8.16 (s, 1H, Ph: H-2), 8.19 (br, 1H, Ph: H-6), 7.40-8.40 (1H, Sq: NH), 9.80 (br, 1H, NH-1); δ_C (75 MHz, DMSO-d_6) 45.7 (C-5′), 46.0 (Bn: CH_2), 71.0 (C-3′), 72.9 (C-2′), 83.7 (C-4′), 87.0 (C-1′), 117.1 (C-5), 122.3 (Ph: C-2), 122.7 (Ph: C-6), 130.6 (Ph: C-5), 134.5 (Ph: C-3), 136.4 (C-8), 141.5 (Ph: C-4), 148.1 (Ph: C-1), 151.6 (C-4), 153.8 (C-2), 157.1 (C-6), 167.6 (Sq: C-4), 182.6 (Sq: C-3), 182.9 (Sq: C-1), 190.2 (Sq: C-2). *m/z* (ESI) 512.1398 ($C_{21}H_{20}N_8O_8$ requires 512.1404).

3-(((2*R*,3*S*,4*R*,5*R*)-5-(2-Amino-6-oxo-1*H*-purin-9(6*H*)-yl)-3,4-dihydroxytetrahydrofuran-2-yl)methylamino)-4-(4-nitrobenzylamino)cyclobut-3-ene-1,2-dione (5e). The title compound was prepared from **3** (50.0 mg, 177 µmol), DIPEA (15.4 µL, 11.4 mg, 88.4 µmol) and **6e** (49.0 mg, 177 µmol) as described for the preparation of **5d**. Thus, **5e** was obtained as a light yellow powder in 74% yield (66.9 mg, 131 µmol): R_f 0.50 (DCM–MeOH–water 7 : 7 : 1); mp 210 °C (decomposition); δ_H (400 MHz, DMSO-d_6) 3.73 (m, 1H, H-5′), 3.96 (m, 1H, H-4′), 4.07 (d, 1H, J = 4.3 Hz, H-3′), 4.52 (m, 1H, H-2′), 4.84 (br, 2H, Bn: CH_2), 5.32 (br, 1H, 3′-OH), 5.55 (d, 1H, J = 4.0 Hz, 2′-OH), 5.72 (d, 1H, J = 4.8 Hz, H-1′), 6.51 (br, 2H, 2-NH_2), 7.58 (br, 2H, Ph: H-3, 5), 7.89 (s, 1H, H-8), 8.24 (br, 2H, Ph: H-2, 6), 7.40-8.40 (2H, 2 × Sq: NH), 9.94 (br, 1H, NH-1); δ_C (75 MHz, DMSO-d_6) 45.8 (C-5′), 46.3 (Bn: CH_2), 71.0 (C-3′), 73.0 (C-2′), 83.7 (C-4′), 87.0 (C-1′), 117.1 (C-5), 124.2 (Ph: C-2, 6), 128.8 (Ph: C-3, 5), 136.4 (C-8), 138.2 (Ph: C-4), 147.1 (Ph: C-1), 151.7 (C-4), 153.9 (C-2), 157.1 (C-6), 162.4 (Sq: C-4), 167.7 (Sq: C-3), 182.6 (Sq: C-1), 184.1 (Sq: C-2). *m/z* (ESI) 512.1397 ($C_{21}H_{20}N_8O_8$ requires 512.1404).

4-(2-(((2*R*,3*S*,4*R*,5*R*)-5-(2-Amino-6-oxo-1*H*-purin-9(6*H*)-yl)-3,4-dihydroxytetrahydrofuran-2-yl)methylamino)-3,4-dioxocyclobut-1-enylamino)butanoic acid (5f). To a solution of **3** (40.0 mg, 142 µmol) in anhydrous DMF (4 mL) were added first DIPEA (12.4 µL, 9.2 mg, 71.2 µmol), and then **6f** (43.2 mg, 190 µmol). The reaction was stirred for seven days at room temperature. The solvent was removed *in vacuo*, and the residue was sonicated with acetone for five minutes. The precipitate was filtered off, washed with acetone and dried at 105 °C to give **5f** as a white powder in 97% yield (63.8 mg, 138 µmol): R_f 0.33 (DCM–MeOH,/water 7 : 7 : 1); mp 242 °C (decomposition); δ_H (400 MHz, DMSO-d_6) 1.73 (br, 2H, Bu: C^3H_2), 2.21 (br, 2H, Bu: C^2H_2), 3.49 (m, 2H, Bu: C^4H_2), 3.72 (m, 1H, H-5′), 3.97 (br, 1H, H-4′), 4.07 (br, 1H, H-3′), 4.52 (m, 1H, H-2′), 5.30-5.60 (br, 2H, 2′-OH, 3′-OH), 5.71 (d, 1H, J = 5.1 Hz, H-1′), 6.57 (br, 2H, 2-NH_2), 7.62 (br, 1H, Sq: NH), 7.89 (s, 1H, H-8), 10.45 (br, 1H, NH-1); δ_C (75 MHz, DMSO-d_6) 26.6 (Bu: C-3), 35.0 (Bu: C-2), 43.1 (Bu: C-4), 45.7 (C-5′), 71.0 (C-3′), 72.9 (C-2′), 83.8 (C-4′), 87.1 (C-1′), 117.2 (C-5), 136.7 (C-8), 149.4 (C-4), 154.0 (C-2), 157.3 (C-6), 168.0 (Sq: C-1), 178.3 (CO_2H), 182.7 (Sq: C-2), 183.6 (Sq: C-4), 188.0 (Sq: C-3). *m/z* (ESI) 463.1450 ($C_{18}H_{21}N_7O_8$ requires 463.1452).

2-(4-(2-(((2*R*,3*S*,4*R*,5*R*)-5-(2-Amino-6-oxo-1*H*-purin-9(6*H*)-yl)-3,4-dihydroxytetrahydrofuran-2-yl)methylamino)-3,4-dioxocyclobut-1-enylamino)methyl)benzoic acid (5g). The title compound was prepared from **3** (40.0 mg, 142 µmol), DIPEA (37 µL, 27.5 mg, 212 µmol) and **6g** (39.0 mg, 142 µmol) as described for the preparation of **5f**. Thus, **5g** was obtained as a white powder in 99% yield (72.1 mg, 141 µmol): R_f 0.58 (DCM–MeOH–water 7 : 7 : 1); mp 267 °C (decomposition); δ_H (400 MHz, DMSO-d_6) 3.67 (m, 1H, H-5′), 3.93 (m, 1H, H-4′), 3.98 (m, 1H, H-5′), 4.06 (br, 1H, H-3′), 4.50 (br, 1H, H-2′), 5.01 (br, 2H, Bn: CH_2), 5.40 (br, 1H, 3′-OH), 5.56 (br, 1H, 2′-OH), 5.69 (d, 1H, J = 6.0 Hz, H-1′), 6.75 (br, 2H, 2-NH_2), 7.28 (br, 0.5H, Sq-NH), 7.35 (m, 3H, Ph: H-3, 4, 5), 7.83 (d, 1H, J = 5.8 Hz, Ph: H-6), 7.86 (s, 1H, H-8), 8.40 (br, 1.5H, Sq-NH), 9.85 (br, 1H, CO_2H), 11.00 (br, 1H, NH-1); δ_C (75 MHz, DMSO-d_6) 45.6 (C-5′), 46.5 (Bn: CH_2), 71.0 (C-3′), 72.9 (C-2′), 83.8 (C-4′), 86.9 (C-1′), 117.1 (C-5), 123.0 (Ph: C-1), 127.6 (Ph: C-4), 129.8 (Ph: C-5), 130.0 (Ph: C-3), 130.6 (Ph: C-6), 136.5 (C-8), 138.1 (Ph: C-2), 151.9 (C-4), 154.1 (C-2), 157.5 (C-6), 168.2 (Sq: C-1), 182.6 (Sq: C-2), 182.8 (CO_2H), 184.3 (Sq: C-4), 189.7 (Sq: C-3). *m/z* (ESI) 511.1445 ($C_{22}H_{21}N_7O_8$ requires 511.1452).

3-(Butylamino)-4-ethoxycyclobut-3-ene-1,2-dione (6a). n-Butylamine (31 µL, 22.9 mg, 0.31 mmol) and DIPEA (30 µl, 22,3 mg, 0.17 mmol) were dissolved in EtOH (1 mL). To the solution, 3,4-diethoxycyclobut-3-ene-1,2-dione (50 µL, 57.5 mg, 0.34 mmol) was added, and the mixture was stirred at room temperature until TLC indicated completion of the reaction (*ca.* 2h). The solvents were removed *in vacuo* and the residue was purified by column chromatography (DCM–MeOH 97.5 : 2.5) to give **6a** as a yellow solid in quantitative yield (61.9 mg, 0.31 mmol): R_f 0.17 (DCM, MeOH 975 : 25); mp 42 °C; δ_H (400 MHz, DMSO-d_6) 0.87 (t, J = 7.2 Hz, 3H, Bu: CH_3), 1.30 (m, 2H, Bu: C^3H_2), 1.36 (t, J = 6.9 Hz, 3H, Et: CH_3), 1.49 (m, 2H, Bu:C^2H_2), 3.29 (t, J = 6.5 Hz, 1H, Bu: C^1H_2), 3.48 (t, J = 7.0 Hz, 1H, Bu: C^1H_2), 4.65 (q, J = 6.9 Hz, 2H, Et: CH_2), 8.59 (br, 0.5H, NH), 8.80 (br, 0.5H, NH); δ_C (75 MHz, DMSO-d_6) 13.6 (Bu: CH_3), 15.8 (Et: CH_3), 19.1 (Bu: C^3H_2), 32.6 (Bu: C^2H_2), 43.5 (Bu: C^1H_2), 69.0 (Et: CH_2), 171.5 (Sq: C-4), 175.6 (Sq: C-3), 182.2 (Sq: C-1), 189.8 (Sq: C-2). *m/z* (ESI) 197.1052 ($C_{10}H_{15}NO_3$ requires 197.1052).

3-(Benzylamino)-4-ethoxycyclobut-3-ene-1,2-dione (6b). n-Benzylamine (37 µL, 36.3 mg, 0.34 mmol) was added at 0 °C to a solution of 3,4-diethoxycyclobut-3-ene-1,2-dione (50 µL, 57.5 mg, 0.34 mmol) in EtOH (2 mL). The reaction was stirred at room temperature overnight. The solvents were removed *in vacuo* and the residue was purified by column chromatography (DCM–MeOH 95 : 5) to give **6b** as a colourless, viscous liquid in 83% yield (64.9 mg, 0.28 mmol): R_f 0.85 (DCM–MeOH 9 : 1); δ_H (400 MHz, $CDCl_3$) 1.42 (t, 3H, J = 7.0 Hz, 6.6 Hz, Et: CH_3), 4.58 (d, 1.5H, J = 5.9 Hz, Bn: CH_2), 4.66 (br, 0.5H, Bn: CH_2), 4.75 (q, 2H, J = 7.0 Hz, 6.6 Hz, Et: CH_2), 7.30 (m, 5H, Ph), 9.08 (br, 0.5H, NH), 9.29 (br, 0.5H, NH); δ_C (75 MHz, $CDCl_3$) 15.6 (Et: CH_3), 48.4 (Bn: CH_2), 69.7 (Et: CH_2), 127.7 (Ph: C-4), 128.1 (Ph: C-2, 6), 128.9 (Ph: C-3, 5), 137.1 (Ph: C-1), 172.5 (Sq: C-3), 177.7 (Sq: C-4), 183.0 (Sq: C-1), 189.6 (Sq: C-2). *m/z* (ESI) 231.0895 ($C_{13}H_{13}NO_3$ requires 231.0895).

3-(2-Nitrobenzylamino)-4-ethoxycyclobut-3-ene-1,2-dione (6c). 2-Nitrobenzylamine hydrochloride (102.2 mg, 0.54 mmol) and DIPEA (140 µL, 103.9 mg, 0.80 mmol) were dissolved in EtOH (5 mL). To the solution, 3,4-diethoxycyclobut-3-ene-1,2-dione (80 µL, 92.0 mg, 0.54 mmol) was added, and the reaction was

stirred at room temperature until TLC indicated completion (*ca.* 2 h). The solvents were removed *in vacuo* and the residue was purified by column chromatography (DCM–MeOH 97.5 : 2.5) to give **6c** as a pale yellow solid in 97% yield (145.4 mg, 0.53 mmol): R_f 0.28 (DCM–MeOH 975 : 25); mp 164 °C; δ_H (400 MHz, DMSO-d_6) 1.23 (t, 1.5H, J = 6.6 Hz, Et: CH_3), 1.38 (t, 1.5H, J = 7.0 Hz, Et: CH_3), 4.55 (q, 1H, J = 7.0 Hz, Et: CH_2), 4.67 (q, 1H, J = 6.6 Hz, Et: CH_2), 4.82 (d, 1H, J = 5.1 Hz, Bn: CH_2), 5.03 (d, 1H, J = 5.1 Hz, Bn: CH_2), 7.60 (m, 2H, J = 7.7 Hz, Ph: H-4, 5), 7.79 (t, 1H, J = 7.7 Hz, 1.1 Hz, Ph: H-3), 8.09 (t, 1H, J = 5.9 Hz, 1.8 Hz, Ph: H-6), 9.07 (t, 0.5H, J = 5.1 Hz, NH), 9.32 (t, 0.5H, J = 5.1 Hz, NH); δ_C (75 MHz, DMSO-d_6) 15.7 (Et: CH_3), 44.4 (Bn: CH_2), 69.4 (Et: CH_2), 125.2 (Ph: C-6), 129.4 (Ph: C-5), 130.1 (Ph: C-3), 133.2 (Ph: C-2), 134.2 (Ph: C-4), 147.9 (Ph: C-1), 173.1 (Sq: C-3), 177.6 (Sq: C-4), 183.0 (Sq: C-2), 189.1 (Sq: C-1). m/z (ESI) 276.0748 ($C_{13}H_{12}N_2O_5$ requires 276.0746).

3-(3-Nitrobenzylamino)-4-ethoxycyclobut-3-ene-1,2-dione (6d). 3-Nitrobenzylamine hydrochloride (100.0 mg, 0.53 mmol) and DIPEA (140 µL, 103.9 mg, 0.80 mmol) were dissolved in EtOH (5 mL). To the solution, 3,4-diethoxycyclobut-3-ene-1,2-dione (78.5 µL, 90.3 mg, 0.53 mmol) was added, and the reaction was stirred at room temperature overnight. The solvents were removed *in vacuo* and the residue was purified by column chromatography (DCM–MeOH 95 : 5) to give **6d** as a pale yellow solid in 65% yield (95.5 mg, 0.35 mmol): R_f 0.39 (DCM–MeOH 95 : 5); mp 113 °C; δ_H (400 MHz, DMSO-d_6) 1.35 (m, 3H, Et: CH_3), 4.64 (m, 2H, Et: CH_2), 4.81 (d, 2H, J = 4.8 Hz, Bn: CH_2), 7.68 (q, 1H, J = 7.7 Hz, Ph: H-5), 7.77 (d, 1H, J = 7.0 Hz, Ph: H-4), 8.17 (d, 1H, J = 7.7 Hz, Ph: H-6), 8.19 (s, 1H, Ph: H-2), 9.15 (br, 0.5H, NH), 9.36 (br, 0.5H, NH); δ_C (75 MHz, DMSO-d_6) 15.5 (Et: CH_3), 46.4 (Bn: CH_2), 69.0 (Et: CH_2), 122.4 (Ph: C-2), 122.6 (Ph: C-6), 130.4 (Ph: C-5), 134.4 (Ph: C-4), 140.5 (Ph: C-3), 148.1 (Ph: C-1), 173.2 (Sq: C-3), 177.5 (Sq: C-4), 183.1 (Sq: C-2), 189.5 (Sq: C-1). m/z (ESI) 276.0748 ($C_{13}H_{12}N_2O_5$ requires 276.0746).

3-(4-Nitrobenzylamino)-4-ethoxycyclobut-3-ene-1,2-dione (6e). 4-Nitrobenzylamine hydrochloride (100.0 mg, 0.53 mmol) and DIPEA (140 µL, 103.9 mg, 0.80 mmol) were dissolved in EtOH (5 mL). To the solution, 3,4-diethoxycyclobut-3-ene-1,2-dione (78.5 µL, 90.3 mg, 0.53 mmol) was added, and the reaction was stirred at room temperature overnight. The solvents were removed *in vacuo* and the residue was purified by column chromatography (DCM–MeOH 95 : 5) to give **6e** as a pale yellow solid in 94% yield (137.5 mg, 0.50 mmol): R_f 0.36 (DCM–MeOH 95 : 5); mp 168 °C; δ_H (400 MHz, DMSO-d_6) 1.29 (t, 1.5H, J = 6.2 Hz, Et: CH_3), 1.37 (t, 1.5H, J = 6.2 Hz, Et: CH_3), 4.65 (m, 2H, Et: CH_2), 4.81 (d, 2H, J = 5.1 Hz, Bn: CH_2), 7.58 (d, 2H, J = 7.7 Hz, Ph: H-3, 5), 8.23 (d, 2H, J = 8.4 Hz, Ph: H-2, 6), 9.16 (t, 0.5H, J = 5.1 Hz, NH), 9.37 (t, 0.5H, J = 5.1 Hz, NH); δ_C (75 MHz, DMSO-d_6) 15.5 (Et: CH_3), 44.6 (Bn: CH_2), 69.0 (Et: CH_2), 123.9 (Ph: C-2, 6), 128.7 (Ph: C-3, 5), 146.3 (Ph: C-4), 147.0 (Ph: C-1), 172.4 (Sq: C-3), 177.8 (Sq: C-4), 181.6 (Sq: C-2), 189.7 (Sq: C-1). m/z (ESI) 276.0748 ($C_{13}H_{12}N_2O_5$ requires 276.0746).

4-(2-Ethoxy-3,4-dioxocyclobut-1-enylamino)butanoic acid (6f). 4-Aminobutanoic acid (50.0 mg, 0.49 mmol) and DIPEA (42 µL, 31.2 mg, 0.24 mmol) were dissolved in MeOH (7 mL). To the solution, 3,4-diethoxycyclobut-3-ene-1,2-dione (72 µL, 82.8 mg, 0.49 mmol) was added, and the reaction was stirred at room temperature overnight. The solvents were removed *in vacuo* and the residue was purified by column chromatography (DCM–MeOH 7 : 3) to give **6f** as a colourless, viscous liquid in 97% yield (106.9 mg, 0.47 mmol): R_f 0.43 (DCM–MeOH 7 : 3); δ_H (400 MHz, DMSO-d_6) 1.38 (m, 3H, Et: CH_3), 1.75 (m, 2H, Bu: C^3H_2), 2.33 (m, 2H, Bu: C^2H_2), 3.49 (br, 2H, Bu: C^4H_2), 4.66 (m, 2H, Et: CH_2), 8.67 (br, 0.4H, NH), 8.84 (br, 0.6H, NH); δ_C (75 MHz, DMSO-d_6) 15.6 (Et: CH_3), 25.4 (Bu: C^3H_2), 30.9 (Bu: C^2H_2), 43.1 (Bu: C^4H_2), 68.7 (Et: CH_2), 172.4 (Sq: C-2), 174.5 (CO_2H), 176.6 (Sq: C-1), 182.1 (Sq: C-3), 189.3 (Sq: C-4). m/z (ESI) 227.0793 ($C_{10}H_{13}NO_5$ requires 227.0794).

2-((2-Ethoxy-3,4-dioxocyclobut-1-enylamino)methyl)benzoic acid (6g). 2-Aminomethylbenzoic acid (100.0 mg, 0.66 mmol) and DIPEA (170 µL, 126.1 mg, 0.98 mmol) were dissolved in MeOH (20 mL). To the solution, 3,4-diethoxycyclobut-3-ene-1,2-dione (98 µL, 112.7 mg, 0.66 mmol) was added, and the reaction was stirred at room temperature overnight. The solvents were removed *in vacuo* and the residue was purified by column chromatography (DCM–MeOH 7 : 3) to give **6g** as a pale orange solid in quantitative yield (181.9 mg, 0.66 mmol): R_f 0.57 (DCM–MeOH 7 : 3); mp 233 °C (decomposition); δ_H (400 MHz, DMSO-d_6) 1.36 (m, 3H, Et: CH_3), 4.63 (m, 2H, Et: CH_2), 4.70 (br, 1H, Bn: CH_2), 4.89 (br, 1H, Bn: CH_2), 7.15-7.45 (m, 4H, Ph: H-3, 4, 5, NH), 7.82 (d, J = 7.3 Hz, 1H, Ph: H-6), 9.64 (br, 1H, CO_2H); δ_C (75 MHz, DMSO-d_6) 15.9 (Et: CH_3), 47.2 (Bn: CH_2), 69.4 (Et: CH_2), 127.7 (Ph: C-5), 128.4 (Ph: C-1), 128.6 (Ph: C-3), 130.0 (Ph: C-4), 130.6 (Ph: C-6), 137.2 (Ph: C-2), 172.4 (Sq: C-2), 176.7 (CO_2H), 177.4 (Sq: C-1), 183.6 (Sq: C-3), 189.3 (Sq: C-4).

3-(2-Nitrobenzylamino)-4-aminocyclobut-3-ene-1,2-dione (7). To a solution of **6c** (30.0 mg, 109 µmol) in MeOH (5 ml) was added aqueous NH_3 (35%, 1mL). The reaction was stirred for two days at 50 °C, by which time TLC indicated complete conversion. The solvent was removed and the residue was recrystallised from methanol to give **7** as a yellow powder in 34% yield (9.0 mg, 36.4 µmol): R_f value: 0.25 (DCM–MeOH 9 : 1); mp 284 °C (decomposition); δ_H (400 MHz, DMSO-d_6) 4.98 (d, 2H, J = 6.2 Hz, CH_2), 7.20-8.05 (br, 3H, NH)7.62 (q, 2H, J = 7.3 Hz, 8.1 Hz, H-3, 5), 7.80 (t, 1H, J = 1.1 Hz, 7.3 Hz, 7.7 Hz, H-4), 8.12 (d, 1H, J = 1.1 Hz, 8.1 Hz, H-6); δ_C (75 MHz, DMSO-d_6) 44.5 (CH_2), 125.4 (C-3), 129.5 (C-4), 131.1 (C-1), 134.1 (C-6), 134.9 (C-5), 147.9 (C-2), 163.8 (Sq: C-3), 172.2 (Sq: C-4), 182.9 (Sq: C-1), 183.3 (Sq: C-2). m/z (ESI) 247.0592 ($C_{21}H_{20}N_8O_8$ requires 247.0593).

2-((1,3-Dioxoisoindolin-2-yl)methyl)benzoic acid. [43] Phthalide (10.00 g, 74.6 mmol) and potassium phthalimide (15.00 g, 81.0 mmol) were suspended in anhydrous DMF (50 mL). The reaction was heated to reflux overnight. After cooling to room temperature, aqueous acetic acid (35%, 80 mL) was added and the reaction was stirred for 30 min. A precipitate formed which was filtered off, washed with water (3 × 20 mL) and EtOH (2 × 20 mL). The precipitate was triturated with boiling aqueous EtOH (60%, 60mL) for 30 min. Hot filtration and washing with EtOH (2 × 10 mL) gave *ca.* 15 g of crude product. This material was recrystallised, in two portions, from glacial acetic acid (300 mL) in the presence of Norit charcoal to give the title compound as a white, crystalline powder in 58% yield (12.15 g, 43.2 mmol): R_f 0.59 (DCM–MeOH 7 : 3); mp 267 °C; δ_H (400 MHz, DMSO-d_6) 5.36

(s, 2H, CH_2), 7.19 (d, 1H, $J = 8.1$ Hz, Bn: H-3), 7.36 (m, 1H, $J =$ 7.3 Hz, 1.1 Hz, Bn: H-4), 7.47 (m, 1H, $J = 7.7$ Hz, 7.3 Hz, 1.1 Hz, Bn: H-5), 7.77 (m, 2H, H-3, H-6), 7.89 (m, 2H, H-4, H-5), 8.08 (dd, 1H, $J = 7.7$ Hz, 1.1 Hz, Bn: H-6); δ_C (75 MHz, DMSO-d_6) 123.4 (Phth: C-2, 5), 126.3 (Ph: C-3), 127.3 (Ph: C-5), 129.2 (Ph: C-1), 130.9 (Ph: C-6), 131.9 (Ph: C-4), 132.6 (Phth: C-1, 6), 134.7 (Phth: C-3, 4), 137.7 (Ph: C-2), 168.2 (2 × C=O), 168.5 (CO_2H).

2-Aminomethylbenzoic acid. [35] 2-((1,3-Dioxoisoindolin-2-yl)methyl)benzoic acid (1.00 g, 3.56 mmol) was suspended in a mixture of anhydrous DMF (7.5 mL) and EtOH (15 mL). The mixture was heated to 75 °C until a clear solution was obtained. To the solution, hydrazine hydrate (64%, 0.5 mL, 7.4 mmol) was added, and the reaction was stirred overnight, at which stage a precipitate had formed. The reaction mixture was cooled for 30 min in an ice bath to complete precipitation. TLC indicated that different from the description in the original protocol[35] the precipitate, and not the filtrate, contained the desired product. The precipitate was filtered off and washed with cold EtOH. The filter cake was dissolved in a small volume of MeOH and loaded onto silica. The silica column was washed with DCM–MeOH (9 : 1) to remove phthalhydrazide, and then eluted with DCM–MeOH–water (7 : 7 : 1). Product-containing fractions were combined and the solvents were evaporated *in vacuo* to give the title compound as a white powder in 44% yield (239 mg, 1.58 mmol): R_f 0.42 (DCM–MeOH–water 7 : 7 : 1); mp 211 °C; δ_H (400 MHz, DMSO) 3.95 (s, 2H, CH_2), 7.27-7.35 (m, 3H, H-3, 4, 5), 7.77 (d, 1H, $J = 7.3$ Hz, H-6), 9.27 (br, 3H, NH_2, CO_2H); δ_C (75 MHz, DMSO-d_6) 44.0 (CH_2), 130.1 (C-5), 130.6 (C-3), 131.6 (C-4), 132.3 (C-1, 6), 141.2 (C-2), 169.6 (CO_2H); *m/z* (ESI) 151.0632 ($C_8H_9NO_2$ requires 151.0633).

NMR titration experiments. ^{1}H NMR titration experiments with $MgCl_2$ were carried out with compounds **5b**, **5c**, **5g**, **6c** and **7** under the following conditions. Test compounds (*ca.* 5–6 μmoles) were dissolved, in separate NMR tubes, in DMF-d_7 (*ca.* 450 mg). To each tube, a solution of $MgCl_2$ in DMF-d_7 (0.35 mmol mg^{-1}) was added in steps corresponding to a total of 0.00 ("blank"), 0.25–2.00 (steps of 0.25), 2.5–4.0 (steps of 0.5), 5, 6, 8 and 10 equivalents of $MgCl_2$. After each addition of $MgCl_2$, ^{1}H NMR spectra were recorded on a Varian VXR 400 S spectrometer at room temperature, until no significant change of the chemical shifts for the NH and NH_2 protons was observed. For data analysis, differences in chemical shift for the NH and NH_2 protons, relative to the "blank" sample, were plotted over the equivalents of $MgCl_2$, as shown in Fig. 5.

Molecular docking. The molecular docking experiments were carried out with AutoDock 3.0.5.[44] The X-ray crystal structure of Kre2p was downloaded from the Protein Data Bank (PDB code 1s4o) and prepared for docking using the AutoDockTools. 1s4o contains the coordinates of yeast alpha1,2-mannosyltransferase in complex with GDP and Mn^{2+},[30] which is thought to be the *in vivo* ion co-factor. Docking parameters were not available for Mn^{2+} in versions of AutoDock prior to 4.0, so a number of available metal ion parameters were evaluated by removing GDP and Mn^{2+} from the PDB file and comparing the docked metal ion position to that of the original Mn^{2+} coordinates. These experiments were performed on chain B using default parameters on a 40 × 30 × 40 grid centered on the Mn^{2+} position. The calcium parameters resulted in the best match so these were used in subsequent dockings that included Mn^{2+}. This choice was validated by docking GDP back into the crystal structure. For the calcium parameters this redocking resulted in large cluster (93 out of 100) of states that fell within 0.1 Å rmsd of the crystal structure coordinates. Ligand geometries were optimised semi-empirically with GAMESS using the AUSTIN MODEL 1 method.[45,46] All dockings were performed on a 60 × 50 × 46 grid of 0.375 Å spacing centred on the known binding site. Two rounds of docking were carried out for each compound using AutoDock's Lamarkian genetic algorithm. A population size of 250 was chosen for the first round and a member from the lowest energy cluster was then fed into the next round as the input structure and optimised within a population of 200.

Recombinant DPMS Assay. Full experimental details will be published elsewhere.[29] Briefly, *E. coli* membranes containing recombinantly expressed, full-length (membrane-bound) *T. brucei* DPMS (70 ng μl^{-1} total protein) was added to a reaction mix (60 μl) of Na-Hepes (50 mM, pH 7.4), KCl (25 mM), $MgCl_2$ (5 mM), $MnCl_2$ (5 mM), didehydrofarnesol-phosphate (1 μg), GDP-[^{3}H]Man (0.25 μCi/1 μM), and potential competing substrate/inhibitor (1 mM unless otherwise stated) all in the presence of 0.1% n-octyl-glucopyranoside and incubated at 30 °C for 10min. The reaction was quenched and lipids extracted by the addition of $CHCl_3$–MeOH (1 : 1) making a final ratio of 10 : 10 : 3 ($CHCl_3$–MeOH–H_2O). The resulting supernatant after centrifugation was dried and partitioned between butan-1-ol and water, a portion butan-1-ol was counted as a measure of didehydrofarnesol-phosphate-[^{3}H]mannose product.

Cytotoxicity studies. The Alamar Blue viability test[40] was used to establish ED_{50} values against cultured bloodstream *T. brucei* (strain 427) for all test compounds.

Acknowledgements

We thank the Norwich Research Park for a studentship, and the UEA and the EPSRC (First Grant EP/D059186/1; to GKW) for financial support. This work was supported in part by a Wellcome Trust Senior Research Fellowship (067441; to TKS). We are grateful to Mr Colin MacDonald for assistance with the NMR experiments, and to the EPSRC National Mass Spectrometry Service Centre, Swansea, for the recording of mass spectra.

References

1 G. K. Wagner, T. Pesnot and R. A. Field, A survey of chemical methods for sugar-nucleotide synthesis, *Nat. Prod. Rep.*, 2009, **26**, 1172–1194.
2 L. L. Lairson, B. Henrissat, G. J. Davies and S. G. Withers, Glycosyltransferases: structures, functions and mechanisms, *Annu. Rev. Biochem.*, 2008, **77**, 521–555.
3 B. Schuman, J. A. Alfaro and S. V. Evans, Glycosyltransferase structure and function, *Top. Curr. Chem.*, 2007, **272**, 217–257.
4 S. Ha, B. Gross and S. E. Walker, *coli* MurG: a paradigm for a superfamily of glycosyltransferases, *Curr. Drug Targets: Infect. Disord.*, 2001, **1**, 201–213.
5 S. Berg, D. Kaur, M. Jackson and P. J. Brennan, The glycosyltransferases of Mycobacterium tuberculosis - roles in the synthesis of arabinogalactan, lipoarabinomannan, and other glycoconjugates, *Glycobiology*, 2007, **17**, 35R–56R.
6 A. J. Schottelius, A. Hamann and K. Asadullah, Role of fucosyltransferases in leukocyte trafficking: major impact for cutaneous immunity, *Trends Immunol.*, 2003, **24**, 101–104.

7 D. H. Dube and C. R. Bertozzi, Glycans in cancer and inflammation: potential for therapeutics and diagnostics, *Nat. Rev. Drug Discovery*, 2005, **4**, 477–488.
8 H. Ko, I. Fricks, A. A. Ivanov, T. K. Harden and K. A. Jacobson, Structure–Activity Relationship of Uridine 5′-Diphosphoglucose Analogues as Agonists of the Human $P2Y_{14}$ Receptor, *J. Med. Chem.*, 2007, **50**, 2030–2039.
9 A. C. Nottbohm and P. J. Hergenrother, Cyclic Compounds as Phosphate Mimics, in *Wiley Encyclopedia of Chemical Biology*, ed. Tadhg P. Begley, Wiley, New York, 2009, **Vol. 3**, pp 661–67610.1002/9780470048672.wecb641.
10 X. Qian, M. M. Palcic, Glycosyltransferase Inhibitors, in *Carbohydrates in Chemistry and Biology*, ed. B. Ernst, G. Hart and P. Sinaÿ; Wiley-VCH, Weinheim, 2000, Part II, Vol. 3; pp 293–312.
11 P. Compain and O. R. Martin, Carbohydrate mimetics-based glycosyltransferase inhibitors, *Bioorg. Med. Chem.*, 2001, **9**, 3077–3092.
12 M. M. Vaghefi, R. J. Bernacki, N. K. Dalley, B. E. Wilson and Robins, R. K., Synthesis of glycopyranosylphosphonate analogs of certain natural nucleoside diphosphate sugars as potential inhibitors of glycosyltransferases, *J. Med. Chem.*, 1987, **30**, 1383–1391.
13 M. M. Vaghefi, R. J. Bernacki, W. J. Hennen and R. K. Robins, Synthesis of certain nucleoside methylenediphosphonate sugars as potential inhibitors of glycosyltransferases, *J. Med. Chem.*, 1987, **30**, 1391–1399.
14 R. R. Schmidt and K. Frische, A new galactosyl transferase inhibitor, *Bioorg. Med. Chem. Lett.*, 1993, **3**, 1747–1750.
15 A. J. Norris, J. P. Whitelegge, M. J. Strouse, K. F. Faull and T. Toyokuni, Inhibition kinetics of carba- and C-fucosyl analogues of GDP-fucose against fucosyltransferase V: implication for the reaction mechanism, *Bioorg. Med. Chem. Lett.*, 2004, **14**, 571–573.
16 S. Vidal, I. Bruyère, A. Malleron, C. Augé and J.-P. Praly, Non-isosteric C-glycosyl analogues of natural nucleotide diphosphate sugars as glycosyltransferase inhibitors, *Bioorg. Med. Chem.*, 2006, **14**, 7293–7301.
17 R. Chang, T.-T. Vo and N. S. Finney, Synthesis of the C1-phosphonate analog of UDP-GlcNAc, *Carbohydr. Res.*, 2006, **341**, 1998–2004.
18 R. Wang, D. H. Steensma, Y. Takaoka, J. W. Yun, T. Kajimoto and C.-H. Wong, A search for pyrophosphate mimics for the development of substrates and inhibitors of glycosyltransferases, *Bioorg. Med. Chem.*, 1997, **5**, 661–672.
19 B. M. Heskamp, G. H. Veeneman, G. A. Van DerMarel, C. A. A. van Broeckel and J. H. van Boom, Design and synthesis of a trisubstrate analogue for α(1→3)fucosyltransferase: A potential inhibitor, *Tetrahedron*, 1995, **51**, 8397–8406.
20 Y. J. Kim, M. Ichikawa and Y. Ichikawa, A rationally designed inhibitor of -1,3-galactosyltransferase, *J. Am. Chem. Soc.*, 1999, **121**, 5829–5830.
21 J. Grugier, J. Xie, I. Duarte and J.-M. Valery, Synthesis of 2-(*N*-acetylamino)-2-deoxy-*C*-glucopyranosyl nucleosides as potential inhibitors of chitin synthases, *J. Org. Chem.*, 2000, **65**, 979–984.
22 L. Ballell, R. J. Young and R. A. Field, Synthesis and evaluation of mimetics of UDP and UDP-α-d-galactose, dTDP and dTDP-α-D-glucose with monosaccharides replacing the key pyrophosphate unit, *Org. Biomol. Chem.*, 2005, **3**, 1109–1115.
23 K. A. Winans and C. R. Bertozzi, An inhibitor of the human UDP-GlcNAc 4-epimerase identified from a uridine-based library: A strategy to inhibit *O*-linked glycosylation, *Chem. Biol.*, 2002, **9**, 113–129.
24 G. Gil-Fernandez, S. Perez, P. Vilas, C. Perez, F. G. De las Heras and A. Garcia Gancedo, Antiviral activity of uridine 5′-diphosphate glucose analogs against some enveloped viruses in cell culture, *Antiviral Res.*, 1987, **8**, 299–310.
25 E. Battaglia, A. Elass, R. D. Drake, P. Paul, S. Treat Magdalou, J. S. Fournle-Gicleux, G. Siest, G. Vergoten, R. Lester and A. Radominska, Characterization of a new class of inhibitors of the recombinant human glucuronosyltransferase, UGT1*6, *Biochim. Biophys. Acta, Gen. Subj.*, 1995, **1243**, 9–14.
26 K. Sato, K. Seio and M. Sekine, Squaryl group as a new mimic of phosphate group in modified oligodeoxynucleotides: Synthesis and properties of new oligodeoxynucleotide analogues containing an internucleotidic squaryldiamide linkage, *J. Am. Chem. Soc.*, 2002, **124**, 12715–12724.
27 K. Seio, T. Miyashita, K. Sato and M. Sekine, Synthesis and properties of new nucleotide analogues possessing squaramide moieties as new phosphate isosteres, *Eur. J. Org. Chem.*, 2005, 5163–5170.
28 T. K. Smith, A. Crossman, J. S. Brimacombe and M. A. J. Ferguson, Chemical validation of GPI biosynthesis as a drug target against African sleeping sickness, *EMBO J.*, 2004, **23**, 4701–4708.
29 J. Nunes, H. Denton, R. T. Schwarz, A. Collier, G. K. Wagner, T. K. Smith, manuscript in preparation.
30 Y. D. Lobsanov, P. A. Romero, B. Sleno, B. Yu, P. Yip, A. Herscovics and P. L. Howell, Structure of Kre2p/Mnt1p: a yeast α1,2-mannosyltransferase involved in mannoprotein biosynthesis, *J. Biol. Chem.*, 2004, **279**, 17921–17931.
31 J. Flint, E. Taylor, M. Yang, D. N. Bolam, L. E. Tailford, C. Martinez-Fleites, E. J. Dodson, B. G. Davis, H. J. Gilbert and G. J. Davies, Structural dissection and high-throughput screening of mannosylglycerate synthase, *Nat. Struct. Mol. Biol.*, 2005, **12**, 608–614.
32 D. K. Dean, An improved synthesis of 5′-amino-5′-deoxyguanosine, *Synth. Commun.*, 2002, **32**, 1517–1521.
33 S. Tomas, R. Prohens, M. Vega, M. C. Rotger, P. M. Deya, P. Ballester and A. Costa, Squaramido-based receptors: Design, synthesis, and application to the recognition of tetraalkylammonium compounds, *J. Org. Chem.*, 1996, **61**, 9394–9401.
34 M. C. Rotger, M. N. Pina, A. Frontera, G. Martorell, P. Ballester, P. M. Deya and A. Costa, Conformational preferences and self-template macrocyclization of squaramide-based foldable modules, *J. Org. Chem.*, 2004, **69**, 2302–2308.
35 J. H. Sun and W. F. Daneker, An efficient synthesis of 2-(((9-fluorenylmethoxycarbonyl)amino)methyl)benzoic acid, *Synth. Commun.*, 1998, **28**, 4525–4530.
36 R. Pink, A. Hudson, M.-A. Mouriès and M. Bendig, Opportunities and Challenges in Antiparasitic Drug Discovery, *Nat. Rev. Drug Discovery*, 2005, **4**, 727–740.
37 K. Nagamune, T. Nozaki, Y. Maeda, K. Ohishi, T. Fukuma, T. Hara, R. T. Schwarz, C. Sutterlin, R. Brun, H. Riezman and T. Kinoshita, Critical roles of glycosylphosphatidylinositol for *Trypanosoma brucei*, *Proc. Natl. Acad. Sci. U. S. A.*, 2000, **97**, 10336–10341.
38 H. Denton, S. Fyffe and T. K Smith, GDP-Man pyrophosphorylase is an essential in bloodstream form *Trypanosoma brucei*, *Biochem. J.*, 2010, **425**, 603–614.
39 T. K. Smith, B. L. Young, H. Denton, D. L. Hughes and G. K. Wagner, First small molecular inhibitors of T. brucei dolichol phosphate mannose synthase (DPMS), a validated drug target in African sleeping sickness, *Bioorg. Med. Chem. Lett.*, 2009, **19**, 1749–1752.
40 J. Mikus and D. Steverding, A simple colorimetric method to screen drug cytotoxicity against *Leishmania* using the dye Alamar Blue, *Parasitol. Int.*, 2000, **48**, 265–269.
41 Y. Sugawara and H. Iwasaki, Structure of disodium uridine diphosphoglucose dihydrate, $C_{15}H_{22}N_2O_{17}P_2^{2-} \times 2\ Na^+ \times 2\ H_2O$, and refinement of dipotassium glucose 1-phosphate dihydrate, $C_6H_{11}O_9P^{2-} \times 2\ K^+ \times 2\ H_2O$ (monoclinic form), *Acta Crystallogr., Sect. C: Cryst. Struct. Commun.*, 1984, **C40**, 389–393.
42 M. A. Macnaughtan, M. Kamar, G. Alvarez-Manilla, A. Venot, J. Glushka, J. M. Pierce and J. H. Prestegard, NMR structural characterization of substrates bound to N-acetylglucosaminyltransferase V, *J. Mol. Biol.*, 2007, **366**, 1266–1281.
43 J. Bornstein, P. E. Drummond and S. F. Bedell, α-Phthalimido-ortho-toluic acid, *Org. Synth.*, 1963, **Coll. Vol. 4**, 810–811.
44 G. M. Morris, D. S. Goodsell, R. S. Halliday, R. Huey, W. E. Hart, R. K. Belew and A. J. Olson, Automated docking using a Lamarckian genetic algorithm and an empirical binding free energy function, *J. Comput. Chem.*, 1998, **19**, 1639–1662.
45 M. J. S. Dewar, E. G. Zoebisch, E. F. Healy and J. J. P. Stewart, The development and use of quantum-mechanical molecular models. Part 76. AM1 – a new general purpose quantum mechanical molecular model, *J. Am. Chem. Soc.*, 1985, **107**, 3902–3909.
46 M. W. Schmidt, K. K. Baldridge, J. A. Boatz, S. T. Elbert, M. S. Gordon, J. H. Jensen, S. Koseki, N. Matsunaga, K. A. Nguyen, S. J. Su, T. L. Windus, M. Dupuis and J. A. Montgomery, General Atomic and Molecular Electronic-Structure System, *J. Comput. Chem.*, 1993, **14**, 1347–1363.
47 A. C. Wallace, R. A. Laskowski and J. M. Thornton, Ligplot – a program to generate schematic diagrams of protein ligand interactions, *Protein Eng., Des. Sel.*, 1995, **8**, 127–134.